Gas-Liquid-Fiber Flow in a Cocurrent Bubble Column

Chengzhi Tang and Theodore J. Heindel
Dept. of Mechanical Engineering, 2025 Black Engineering Building, Iowa State University, Ames, IA 50011

DOI 10.1002/aic.10496
Published online July 18, 2005 in Wiley InterScience (www.interscience.wiley.com).

Effects of superficial gas velocity ($U_l \leq$ *10 cm/s), superficial liquid velocity (*$U_g \leq$ *10 cm/s), and fiber mass fraction (*$0 \leq C \leq$ *2%) on gas holdup (*ε*) and flow regime transition are studied experimentally in well-mixed water-cellulose fiber suspensions in a cocurrent bubble column. Experimental results show that gas holdup decreases with increasing superficial liquid velocity when fiber mass fraction and superficial gas velocity are constant. Gas holdup is not significantly affected by fiber mass fraction in the range of* $C <$ *0.4%, but decreases with increasing fiber mass fraction in the range of* $0.4\% \leq C \leq$ *1.5%. The mechanisms behind the influences of superficial liquid velocity and fiber mass fraction on gas holdup in a gas-liquid-fiber bubble column are analyzed. The effects of gas distribution methods are also explained by comparison to previous results. The axial gas holdup distribution is shown to be a complex function of superficial gas and liquid velocities and fiber mass fraction. The drift-flux model is used to identify the flow regime transitions at different operating conditions. Three distinct flow regimes are observed when* $C \leq$ *0.4%, but only two are identified when* $0.6\% \leq C \leq$ *1.5%. The superficial gas velocities at which the flow transitions from one regime to another are not significantly affected by* U_l*, and only slightly decrease with increasing* C*.* © 2005 American Institute of Chemical Engineers *AIChE J,* 51: 2665–2674, 2005

Keywords: bubble column, cellulose fiber, drift flux, gas holdup, hydrodynamics, multiphase flow

Introduction

Gas-liquid-cellulose fiber systems are found in the pulp and paper industry in a variety of unit operations including flotation deinking, direct-contact steam heating, gaseous fiber bleaching and papermaking.[1] In processes such as flotation deinking, direct-contact steam heating, and bleaching, gases are intentionally introduced into the system, and it is important to create a homogeneous mixture with sufficient interfacial area for mass and/or heat transfer. In contrast, deaeration is used to remove unwanted gas from the system.

Water-cellulose fiber systems are unique because cellulose fiber has a density close to that of water. A water-fiber suspension is also considered a pseudoplastic fluid,[2,3] which acts as a non-Newtonian fluid above a shear stress threshold and acts as a solid otherwise. The shear stress threshold has been shown to increase with fiber mass fraction.[2,3] Fiber suspensions also have a tendency to form regions where the fibers aggregate (that is, flocculate) at fiber mass fractions as low as $C = 0.3\%$ and continuous fiber networks when $C \geq 1\%$.[4] Factors affecting floc formation and deformation include flow conditions, fiber length, and fiber stiffness.[3] Robertson and Mason[5] showed that floc size could be affected by the turbulence intensity of fully developed flows, and by the decay rate of turbulence in the flow. It has also been shown that floc size depends on turbulent eddy size, and small eddies are required to create small flocs.[6]

Numerous fiber suspension flow studies have shown that the presence of fibers significantly suppress small-scale velocity fluctuations.[7–10] Norman et al.[7] suggested fibers damp the turbulence intensity by supplying a force-bearing link between

Correspondence concerning this article should be addressed to T. J. Heindel at theindel@iastate.edu.

nearby fluid elements moving at different velocities, and, thus, suppressing the velocity difference. Increasing the fiber mass fraction, length, and flexibility resulted in a higher reduction in the turbulence intensity. Steen[8] showed that the turbulence structure in fiber suspension pipe flow was changed due to the presence of fibers, and the change was related to the crowding factor (N), which is defined as the number of fibers in a volume swept out by the length of a single fiber.[4] For most situations, the turbulence intensity was reduced, primarily at small length scales. The turbulence intensity increased in the small length scales only when the crowding factor was small (for example, $N \approx 3.6$), or when the crowding factor was in the medium range and the flow was in the wall region. The suppression of the small-scale components of the turbulence spectrum by fiber addition was also reported by Andersson and Rasmuson[9] and Forgacs et al.,[10] who further concluded that the suppression was stronger at higher fiber mass fractions.

In previous gas-liquid-cellulose fiber cocurrent bubble columns studies, gas holdup was found to increase with increasing superficial gas velocity.[11–13] The effect of superficial liquid velocity on gas holdup was found to be rather complex. Lindsay et al.[11] reported superficial liquid velocity had a negligible effect on gas holdup in an air-water two-phase cocurrent bubble column with a 12.7 cm dia. Using the same column, Schulz and Heindel[12] concluded that the cross-sectional averaged gas holdup at a low column position increased with superficial liquid velocity ($2.5 \leq U_l \leq 7.5$ cm/s) at all studied fiber mass fractions, while this was observed only at an intermediate fiber mass fraction at a higher column position. Using a 5.1 cm dia. cocurrent bubble column, Xie et al.[13] reported gas holdup decreased with increasing superficial liquid velocity when $21 \leq U_l \leq 51$ cm/s.

The effect of fiber mass fraction on gas holdup in a cocurrent gas-liquid-cellulose fiber system has also been shown to be complicated. Lindsay et al.[11] reported that when their system contained $C = 1\%$ fiber, gas holdup was higher than that of the column filled with water under the same flow conditions. Studying $C = 0$, 0.8%, and 1.2% fiber systems, Schulz and Heindel[12] showed that the column-average gas holdup was highest at $C = 0.8\%$ and lowest at $C = 1.2\%$ when all other conditions were constant. This was also observed by Xie et al.[13] in their 5.1 dia. column. It is reasonable to consider that the highest gas holdup obtained at the intermediate fiber mass fraction in a cocurrent bubble column was due to some complex interactions between superficial liquid velocity, and fiber mass fraction because gas holdup has been shown to decrease with increasing fiber mass fraction in semibatch bubble columns, and this decrease was attributed to fiber enhanced bubble coalescence.[11,14–16]

Several investigators have studied gas flow regime changes in gas-liquid-cellulose fiber bubble columns. Walmsley[17] observed bubbly flow and churn-turbulent flow in a 2-D semibatch column, and two 3-D semibatch columns of different aspect ratios. Lindsay et al.[11] recorded bubbly flow and churn-turbulent flow in a 12.7 cm semibatch bubble column, and a 12.7 cm cocurrent bubble column with $C = 1\%$ or 2%. Reese et al.[16] found that in a 10.2 dia. cylindrical semibatch bubble column filled with a fiber suspension, dispersed bubble, vortical-spiral, and turbulent flow could be identified when the fiber mass fraction was low ($C \leq 0.5\%$), while only dispersed bubble and turbulent flow were recorded at high fiber mass fractions ($C > 0.5\%$). In a 1 m tall 2-D semibatch bubble column with a rectangular cross-section of 20 cm $\times$ 2 cm, Heindel[18] observed vortical, churn-turbulent, surge churn-turbulent, and discrete channel flow as the fiber mass fraction increased from 0% to 5% with a fixed superficial gas velocity of 0.83 cm/s. In a 1.80 m tall 5.1 cm diameter cocurrent bubble column, Xie et al.[13] recorded five distinct flow regimes in an air-water-cellulose fiber suspension, including dispersed bubbly, layered bubbly, (incipient plug and) plug, churn-turbulent, and slug flows. The superficial gas velocity at which flow regime transition occurred decreased with fiber addition.[11,13,17,19]

In both semibatch[11] and cocurrent bubble columns,[11,12] the cross-sectional average gas holdup was reported to increase with increasing vertical distance from the column bottom and was attributed to fiber suspension recirculation near the column top. Schulz and Heindel[12] observed that the increase in cross-sectional average gas holdup with position was enhanced with increasing superficial gas velocity when $U_g > 2.0$ cm/s.

In this article, a detailed experimental study of superficial liquid velocity, superficial gas velocity, and fiber mass fraction on gas holdup, axial gas holdup variation, and flow regime transition in well-mixed air-water-cellulose fiber suspensions are reported for $U_l \leq 10$ cm/s, $U_g \leq 22$ cm/s, and $C \leq 2\%$. Effects of gas distribution methods on hydrodynamics and gas holdup are also analyzed while comparing the results with previous investigations.

Experimental Procedures

The experiments for this study are conducted in a cylindrical cocurrent bubble column, which consists of four 0.914 m tall acrylic tubes with 15.24 cm internal dia. Five delrin collars, each 5.1 cm tall, and 11 buna-n gaskets are used to connect the acrylic tubes for a total column height of 4 m. Figure 1 shows the entire system. Filtered air is supplied by a compressor and enters the bubble column from the bottom via a spider sparger. The air flow rate is adjusted with a regulator and measured with one of three gas flowmeters (Aalborg, Model: GFM 371s, 471, and 671s, respectively), each covering a different flow rate range. The fiber suspension from a 379 L reservoir is pumped into the column. The pump is connected to the reservoir with a 2.44 m long 7.62 cm diameter PVC pipe. A 2.85 m long 2.54 cm dia. PVC pipe connects the pump to the column. The fiber suspension flow rate is measured with a magnetic flowmeter (COPA-XE™ Series 4000, Model: 10DX4311) and varied via a pump power frequency controller. The fiber suspension enters the column through a flow expander to provide a nearly uniform liquid velocity field at the entrance region prior to the spider sparger. A gas-liquid separator is located on top of the column where air is separated from the water while the water returns to the reservoir through a PVC pipe. Along the column, 5 pressure transducers (Cole-Parmer, Model: 68075, labeled as P_1, P_2, P_3, P_4, and P_5 in Figure 1) are installed, one in each of the five delrin collars. Each acrylic tube section is numbered 1 to 4 from the bottom of the column. Two type-T thermocouples are also located at the bottom and top of the column, respectively. All pressure, flowmeter, and thermocouple signals are collected via a computer controlled data acquisition system. Superficial gas and liquid velocities are controlled by a gas regulator and pump power frequency controller, respectively.

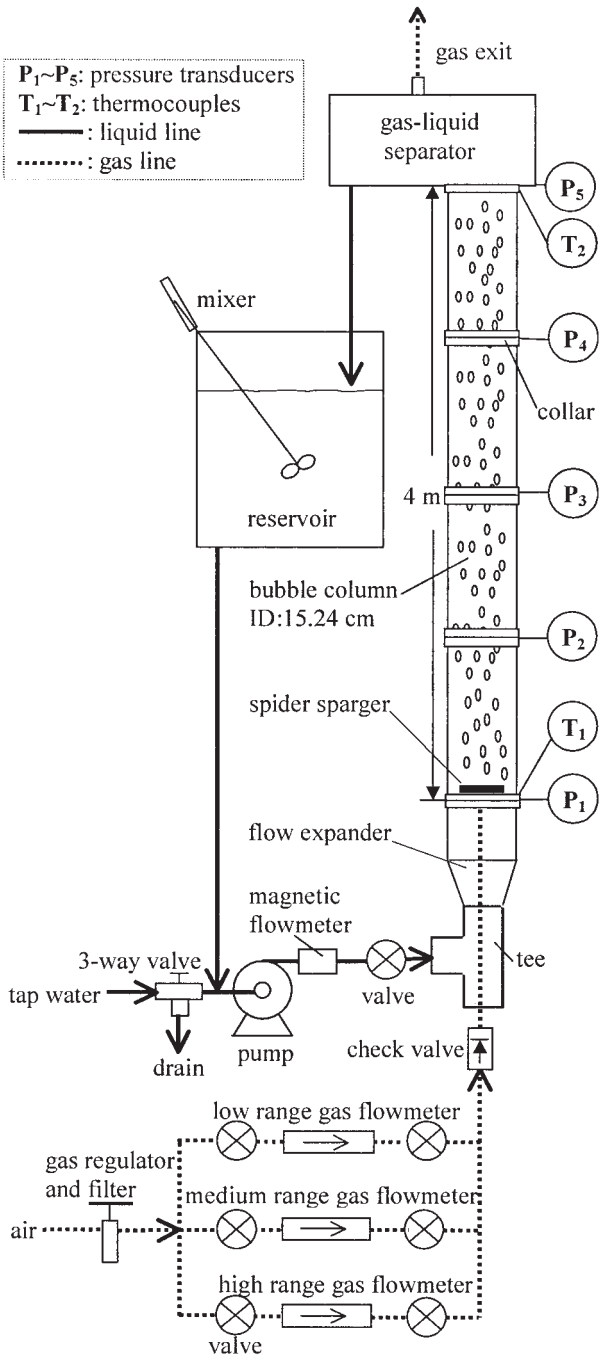

Figure 1. Cocurrent bubble column experimental facility.

The spider sparger, shown in Figure 2, has eight arms made of 12.7 mm dia. stainless steel tubes. Thirty-three 1.6 mm dia. holes are located on one side of each arm and distributed as shown in Figure 2. The arms are soldered to the center cylinder of the sparger such that all the holes face the same direction. Air enters the spider sparger from the central cylinder and exits from the arm holes. The sparger is installed with the holes facing upward.

All experiments in this study are carried out under atmospheric pressure and ambient temperature. The superficial gas velocity range is 0 cm/s $\leq U_g \leq$ 22 cm/s, and the superficial liquid velocity range is 0 cm/s $\leq U_l \leq$ 10 cm/s. Eucalyptus wood fiber and tap water comprise the fiber suspension. The fibers have a length-weighted average fiber length of ~0.8 mm and a fiber coarseness index of ~7.2 mg/100 m. All fiber is disintegrated from dry lap fiber sheets. The fiber sheets are originally torn into small pieces and then a specified mass of oven-dry fiber is weighed. It is then soaked in tap water for 24 h before the pieces of fiber sheet are disintegrated in a Black-Clawson laboratory hydropulper. The concentrated fiber suspension is then transferred to the reservoir and additional tap water is added to raise the suspension to a predetermined level. Fiber mass fraction C is defined as the ratio of the oven-dry fiber mass to the suspension mass.

To acquire gas holdup data at a given U_g and U_l, 4,800 readings are collected from each instrument every 10 ms, and averaged after quasi-steady conditions are reached. With five pressure signals, the time-averaged gas holdup in each section is calculated from

$$\varepsilon_i = 1 - \frac{\Delta p_i}{\Delta p_{0,i}} \tag{1}$$

where $\Delta p_i = p_{L,i} - p_{H,i}$ is the pressure difference between the lower ($p_{L,i}$) and higher ($p_{H,i}$) ends of column section i (i = 1, 2, 3, 4); $\Delta p_{0,i}$ is the corresponding pressure difference when the column is filled only with the specified water-fiber suspension flowing at the same U_l. Equation 1 accounts for the effects of wall shear stress, but neglects the effect of liquid acceleration due to void changes that may influence gas holdup in cocurrent bubble columns;[20–22] however, these effects are estimated to be negligible for the conditions of this study. The overall column gas holdup is defined as $\varepsilon = (\varepsilon_1 + \varepsilon_2 + \varepsilon_3)/3$, the average gas holdup in the three lower sections. The gas holdup in the top section is not included in the overall gas holdup because of measurement error due to the void caused by large bubbles escaping the column top, which is significant during some experimental conditions (see details in the following results).

The typical uncertainties associated with superficial velocities are ±2~4% for U_g and ±1.5~5% for U_l, respectively.

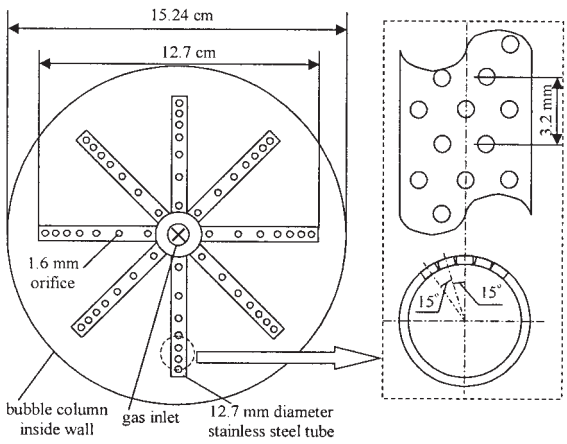

Figure 2. Spider sparger.

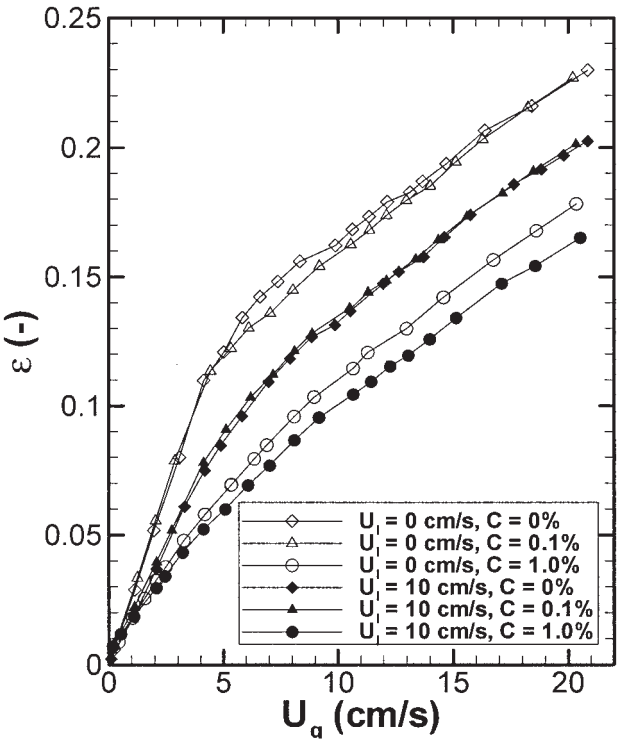

Figure 3. Variation of gas holdup with superficial gas velocity at different superficial liquid velocities and fiber mass fractions.

The corresponding absolute gas holdup uncertainty is estimated to be $\Delta\varepsilon \approx \pm 0.005 \sim 0.01$.

Results and Dicussions

Effect of superficial gas velocity

Figure 3 shows the variation of ε with U_g at different U_l and C in a cocurrent bubble column. Gas holdup increases with increasing U_g for all conditions addressed in this study. There is no local gas holdup maximum, which is observed at low fiber mass fractions in a 15.24 cm air-water-Rayon fiber semibatch bubble column with a perforated plate gas distributor.[15] At low fiber mass fractions ($C = 0.1\%$), the gas holdup is similar to that of an air-water system ($C = 0\%$). When $U_g \lesssim 4$ cm/s, gas holdup increases proportionally with U_g. At $U_g \approx 0$ cm/s, gas holdup is very close to zero, suggesting no air entrainment in the fiber suspension. When $U_g \gtrsim 13$ cm/s, gas holdup increases with U_g, but the slope is less than that when $U_g \lesssim 4$ cm/s. At high fiber mass fractions ($C = 1.0\%$), gas holdup also increases with U_g. At $U_g \approx 0$ cm/s, gas holdup is nonzero but small, due to a small amount of air entrained in the fiber suspension ($\varepsilon \approx 0.005$). The small amount of entrained air can actually be observed in the pump suction line. Similar results were reported by Lindsay et al.[11] and were attributed to the same reason.

Effect of superficial liquid velocity

Generally, gas holdup decreases with increasing U_l providing U_g and C are constant. Figures 3 compares the results at $U_l = 0$ and 10 cm/s for $C = 0\%$, 0.1% and 1.0%. The effect of U_l on ε is similar when $C = 0.1\%$ and 0%. When $C = 1.0\%$, the gas holdup decrease from $U_l = 0$ cm/s to $U_l = 10$ cm/s is significantly smaller than that at $C = 0.1\%$ or 0%. Figure 4 shows that ε linearly decreases with increasing U_l at $0 \le C \le 1.5\%$ when $U_g = 13$ cm/s; the decrease is attributed to the bubble residence time decrease due to increasing superficial liquid velocity. It is also shown that the effect of U_l on ε is more evident at lower C. This can be explained by the fact that the number of large bubbles increases with increasing fiber mass fraction.[23] Large bubbles dominate the flow in the bubble column at the higher fiber mass fractions and have a much smaller residence time. Increasing the superficial liquid velocity does not significantly decrease their residence time.

The effect of U_l on ε in this study agrees with the results reported by Xie et al.[13] for the cross-sectional average gas holdup in a 5.08 cm cocurrent bubble column filled with a kraft softwood fiber suspension and 21 cm/s $\le U_l \le$ 51 cm/s. However, Schulz and Heindel[12] reported that the cross-sectional average gas holdup increased with increasing U_l (2.5 cm/s $\le U_l \le$ 7.5 cm/s) when $C = 0\%$, 0.8% or 1.2% at a lower position ($H = 50.8$ cm), but this trend was significant only when $C = 0.8\%$ at a higher position ($H = 132.1$ cm) in a 12.7 cm dia. cocurrent bubble column using old newspaper fiber. The difference in results is attributed to the method of gas distribution.

Schulz and Heindel[12] used forced air injection where air was dispersed by shear into the fiber suspension in a 2.5 cm pipe prior to a conical diffuser at the bottom of the bubble column. With this method, bubbles that are formed in the 2.5 cm pipe are carried away by the fiber suspension right after they are

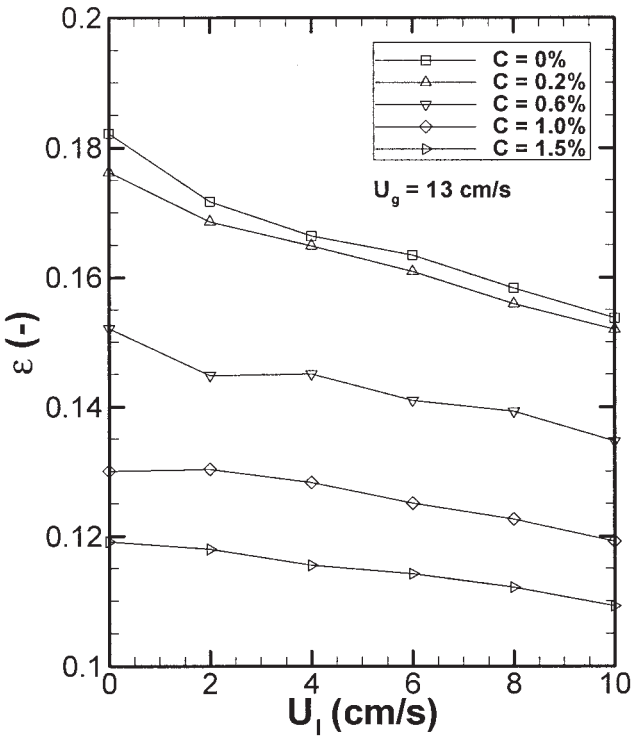

Figure 4. Variation of gas holdup with superficial liquid velocity at different fiber mass fractions (U_g = 13 cm/s).

released. The velocity of the fiber suspension in the 2.5 cm pipe is about 0.625 m/s to 1.875 m/s when 2.5 cm/s $\leq U_l \leq$ 7.5 cm/s. As a result, bubbles are uniformly distributed in the fiber suspension and bubble coalescence after gas injection is minimized. Bubble coalescence is further inhibited by the presence of fiber networks, which work as separating "walls" between bubbles. The effective thickness of the "walls" is larger at higher fiber suspension flow rates (that is, the relative bubble rise velocity is minimized).

Furthermore, it is well documented that when bubbles form in a liquid cross-flow, bubble size decreases significantly with increasing liquid velocity.[24–27] Maier[24] reported that bubble size decreased with increasing cross-flow velocity, typically by a factor of about 3, over the liquid velocity range 0–3.74 m/s. Johnson et al.[25] proposed a model indicating that the equivalent diameter of the bubbles decreased significantly with increasing liquid cross-flow velocity. Waldie et al.[26] found that the Sauter mean diameter of bubbles formed in a liquid cross-flow was proportional to $V_c^{-1.64}$, where V_c is the liquid cross-flow velocity. Forrester and Rielly[27] reported that increasing the liquid cross-flow velocity resulted in a significant decrease in the bubble size between a liquid velocity of 1 and 3 m/s for a constant gas injection flow rate, and further increases in the liquid velocity had a much smaller effect on bubble size.

As a result, the smaller bubbles formed in the entrance region of Schulz and Heindel[12] coupled with the large effective separating "wall" thickness found in fiber suspensions, increased gas holdup with increasing U_l.

As the bubbles and fiber suspension flow upward along the bubble column, more and more bubble-bubble interaction is observed, resulting in bubble coalescence. At higher positions in the column, bubble coalescence dominates the flow. The resulting large bubbles have a very large velocity. Hence, the relative bubble rise velocity is sufficient to be unaffected by the superficial liquid velocity. As a result, the effect of superficial liquid velocity on gas holdup at high positions is less significant than at low positions. This explanation also agrees with the result of Schulz and Heindel[12] that the effect of superficial liquid velocity on gas holdup was more evident at lower positions of the bubble column, where the entering bubble size had a significant influence on the gas holdup.

Xie et al.[13] used a hydrosonic mixer to create gas-liquid mixing. Gas was first introduced to the liquid line and relatively large bubbles were formed. They then flowed with the liquid phase into the hydrosonic mixer, where the large bubbles were broken by a specially designed rotating disk, creating millions of uniformly distributed microbubbles due to cavitation and a cavitation induced shock wave.[28] When the well-mixed gas-liquid mixture exited the mixer, the microbubbles began to agglomerate into larger bubbles. The agglomeration of microbubbles is homogeneous inside the suspension, and when the bubble size is larger than the fiber spacing, bubble movement is confined by the fiber network and bubble agglomeration stops. The agglomeration process of microbubbles is not significantly affected by the liquid velocity because the process occurs at a length scale smaller than that of fiber flocs, most of which flow in their entireties. As a result, the gas holdup decreases with increasing U_l due to a decrease in bubble residence time.

In the current study, however, air is released from a spider sparger with uniformly distributed 1.6 mm holes at the bottom of the bubble column after the water-fiber suspension enters the column. The gas exits the sparger holes in the same direction as the liquid. Under most operating conditions, the bubble rise velocity at release from the sparger holes is higher than the suspension velocity. This, and the liquid circulation in the bubble column, which makes released bubbles migrate toward the column center,[29,30] result in bubble coalescence. The presence of fiber networks significantly enhances bubble coalescence. At higher fiber mass fractions, bubble coalescence occurs right above the sparger. Increasing U_l in the range of 0 cm/s $\leq U_l \leq$ 10 cm/s does not provide a uniform bubble distribution in the fiber suspension. Hence, the decrease in gas holdup due to a decreasing bubble residence time with increasing U_l is not offset by the potential gas holdup increase due to the inhibition of bubble coalescence by increasing U_l.

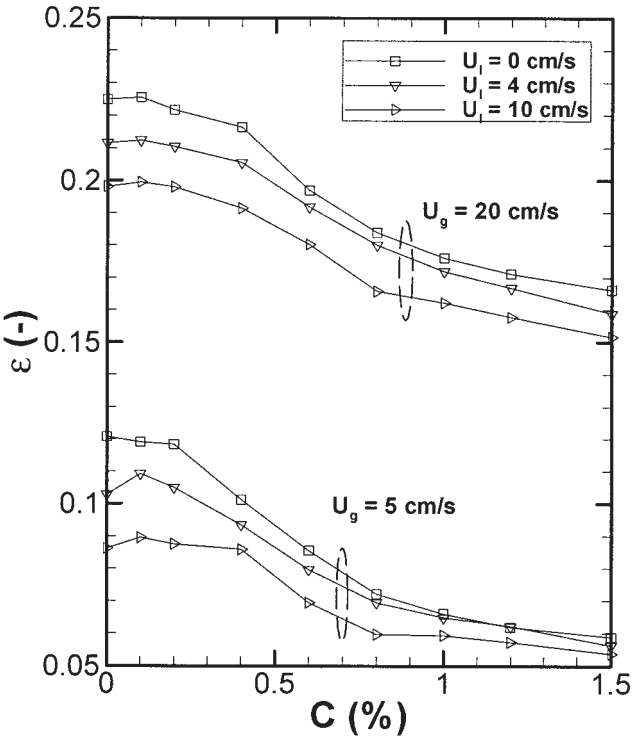

Figure 5. Variation of gas holdup with fiber mass fraction at different superficial liquid velocities.

Effect of fiber mass fraction

Figure 5 shows the effect of fiber mass fraction ($0 \leq C \leq 1.5\%$) on gas holdup at different superficial liquid velocities (U_l = 0, 4, or 10 cm/s) and superficial gas velocities (U_g = 5 or 20 cm/s). Data have also been acquired at $C = 2.0\%$, but are not presented here because the gas holdup does not follow the general trend due to significant gas entrainment in the fiber suspension; significant gas entrainment is not observed at any other fiber mass fraction.[31] When $C \leq 0.2\%$, the influence of fiber mass fraction on gas holdup is insignificant. This is because at $C = 0.1\%$ and 0.2%, fiber flocculation does not occur and bubble movement in the fiber suspension is similar to that of water. When $0.4\% \leq C \leq 1.5\%$, ε decreases significantly with increasing C providing U_g and U_l are constant, and this is attributed to fiber flocculation. As fibers

flocculate, bubble movement near the sparger is retarded by the fiber network, resulting in enhanced coalescence between leading and trailing bubbles. This is supported by observations of Ajersch and Pelton[32] and Walmsley.[17] As a result, much larger bubbles appear at lower column positions[23,33] and they rise faster reducing gas holdup. The resistance to bubble movement resulting from fiber network formation increases with fiber mass fraction, thus, the gas holdup decreases significantly with increasing fiber mass fraction.

The presence of fibers also reduces the gas holdup by inhibiting bubble breakup. It is widely accepted that in turbulent flow fields, only eddies of scales close to the bubble diameter are capable of causing large bubble deformation and breakup; larger eddies merely transport the bubbles.[34–37] As fibers are added, small-scale eddies are suppressed and the suppression is stronger at higher fiber mass fraction.[7–10] Hence, bubble shape is affected and bubble breakup is reduced in fiber suspensions. This is supported by observation of Heindel and Monefeldt[19] that the bubbles in a $C = 0.5\%$ fiber suspension were more spherical than those in pure water in the same semibatch bubble column.

It also noticed from Figure 5 that the gas holdup decrease with increasing fiber mass fraction is less severe at $1.2\% \leq C \leq 1.5\%$ than that at $0.4\% \leq C \leq 1.0\%$. This is attributed to 2 factors: (1) the amount of entrained gas in the fiber suspension increases with increasing fiber mass fraction and compensates for the decrease in gas holdup due to increasing fiber mass fraction, and (2) when $C \geq 1.2\%$, most newly generated bubbles coalesce in the aeration zone so increasing fiber mass fraction does not enhance bubble coalescence as effectively as the same increase in fiber mass fraction in the range of $0.4\% \leq C \leq 1.0\%$.

As shown in Figure 5, at $U_g = 20$ cm/s, ε decreases with C in the same manner for all U_l, indicating a negligible influence of U_l on the effects of fiber mass fraction at high superficial gas velocities. However, when $U_g = 5$ cm/s and $C \geq 1.0\%$, all gas holdup values converge. The difference is attributed to the effect of the suspension flow. When $U_g = 20$ cm/s, a large number of bubbles are released from the sparger holes with velocities higher than the suspension velocity. Significant bubble coalescence and backmixing occurs at all superficial liquid velocities. Thus, increasing fiber mass fraction at each U_l results in a similar gas holdup variation. When $U_g = 5$ cm/s, only a small number of bubbles are released from the sparger holes and their velocity is small. At zero and low superficial liquid velocities, bubble velocity is higher than the suspension velocity. Bubble coalescence and backmixing is significant. Thus, increasing fiber mass fraction results in a similar gas holdup variation as the trend observed at $U_g = 20$ cm/s. At high superficial liquid velocities, the bubble velocity is lower than the suspension velocity. Bubbles are carried away from the sparger and bubble coalescence and backmixing is inhibited. Increasing C does not significantly affect bubble coalescence. Furthermore, loss in gas holdup due to a decrease in the bubble residence time at higher U_l is offset by the gain in gas holdup due to inhibition of bubble coalescence. As a result, the gas holdup difference between $U_l = 0$, 4, and 10 cm/s decreases with increasing C.

It is noticed that the trend of gas holdup variation with fiber mass fraction in this study is different from the observations of Lindsay et al.,[11] Schulz and Heindel,[12] and Xie et al.,[13] where they all reported that gas holdup increased with increasing fiber mass fraction in cocurrent bubble columns in certain ranges of fiber mass fractions. Lindsay et al.[11] observed gas holdup at $C = 1\%$ was higher than that at $C = 0\%$ when $U_l = 2.5$ cm/s or 5 cm/s. Using the same bubble column, Schulz and Heindel[12] observed cross-sectional average gas holdup reached its maximum when $C = 0.8\%$. Xie et al.[13] reported that cross-sectional gas holdup in a 5.08 cm cocurrent bubble column was much higher when $C = 1.0\%$ or 1.5% than $C = 0.5\%$. The difference is mainly caused by the different gas distribution methods used in the studies. Lindsay et al.[11] and Schulz and Heindel[12] used a forced air injection method, while Xie et al.[13] used a hydrosonic pump to mix air into the fiber suspension. Both methods are described in the previous section. One important characteristic of both gas distribution methods is that gas can be uniformly distributed in the fiber suspension and bubble coalescence at the bubble column entrance region is inhibited. At higher fiber mass fractions, the fiber network strength and, thus, the inhibition of bubble coalescence is stronger, when well-dispersed bubbles are initially present in the suspension.

The decrease in gas holdup observed by Schulz and Heindel[12] when C was increased from 0.8% to 1.2% is not fully understood. One possible explanation is that when $C = 1.2\%$, the fiber network was strong such that the high velocity air-suspension mixture from the 2.5 cm pipe was not uniformly distributed via the conical expansion, which was assumed to occurred at $C = 0.8\%$. This may have caused channeling in the entrance region (bubbles travel in a preferential path), resulting in enhanced bubble coalescence and the corresponding reduced gas holdup.

Axial gas holdup variation

Figure 6 presents the sectional average gas holdup distribution at different superficial liquid velocities when $U_g = 18.5$ cm/s and $C = 0.1\%$ or 1.0%. Generally, the difference between the sectional average gas holdups in sections 2 and 3 is much less significant than that between sections 1 and 2, or sections 3 and 4. The average gas holdup in section 1 is significantly lower because in section 1, especially in the region right above the sparger, bubbles flow upward rather fast with paths less tortuous than those in sections 2–4, where gas backmixing is significant, which enhances bubble residence time. It is also noticed that the difference between ε_1 and ε_2 increases with increasing U_l, particularly at low fiber mass fractions (for example, $C = 0.1\%$). This is due to shorter bubble residence time in section 1 at higher U_l.

The higher average gas holdup in section 4 than that in section 3 can be attributed to two reasons: (1) large voids that are formed when large bubbles are violently released at the top of the column; and (2) small bubbles are entrained from the column exit and carried downward with backmixed liquid.[11,12] At low fiber mass fractions (that is, $C = 0.1\%$), flocculation is insignificant and no fiber networks form, thus, bubble entrainment at the column exit is insignificant, but the void formation at the column exit is very significant at high superficial gas velocities (for example, $U_g = 18.5$ cm/s). When the large voids form, they temporarily reduce the liquid surface in the bubble column to a height below pressure transducer P_5 for a time period that decreases with increasing U_l. If the super-

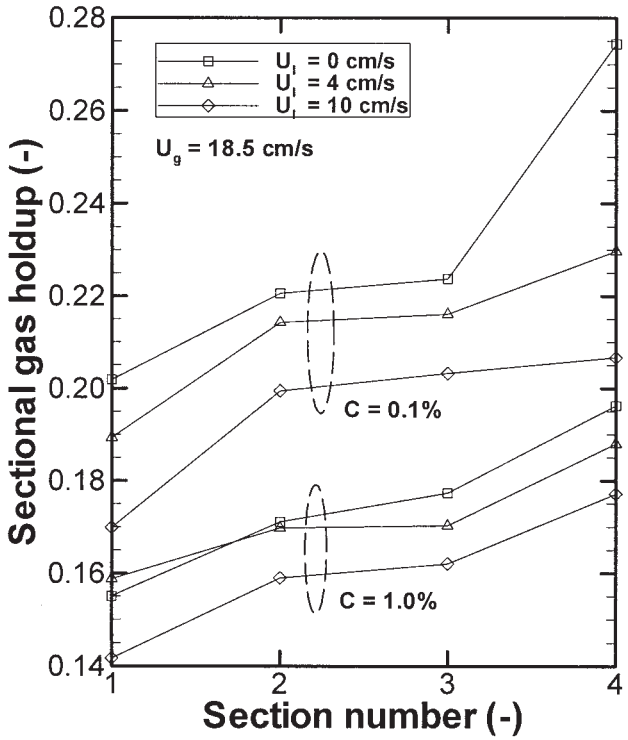

Figure 6. Axial gas holdup variation at different superficial liquid velocities and fiber mass fractions (U_g = 18.5 cm/s).

ficial liquid velocity is smaller than a critical value, the time period is long enough to produce a significant error in ε_4 due to the liquid height being below P_5. The error makes the ε_4 larger than its real value, and it increases with decreasing superficial liquid velocity, as shown in Figure 6. When the superficial liquid velocity is sufficiently large (for example, U_l = 10 cm/s, Figure 6), the voids are quickly filled by liquid upflow, making the error less significant. The gas holdup error due to void formation at the column exit is the reason that ε_4 is not included in the average column gas holdup. At high fiber mass fractions (for example, C = 1.0%), fiber network formation and bubble entrainment at the column exit is significant. This influences ε_4 most because the entrained small bubbles coalesce with other bubbles and rise, and only a small fraction of the small bubbles migrate to lower column sections. Additionally, visual observations for C = 1% reveal pressure transducer P_5 is seldom exposed to air (that is, the large bubble release is less violent at the higher fiber mass fractions). Hence, $\varepsilon_3 - \varepsilon_4$ does not change with superficial liquid velocity at C = 1% (Figure 6).

Figure 7 compares the average gas holdups in sections 1, 2, and 3, as a function of fiber mass fraction at U_l = 8 cm/s. The difference between gas holdup in sections 2 and 3 is negligible when U_g = 5 cm/s, but is apparent and increases slightly with fiber mass fraction when U_g = 18 cm/s and $C \geq 0.6\%$. This is due to bubble entrainment, which is insignificant when U_g = 5 cm/s for all $C \leq 1.5$, but is significant and increases with increasing fiber mass fraction when U_g = 18 cm/s and $C \geq 0.6\%$. As indicated in Figure 7, the gas holdup in section 1 is significantly lower than that in sections 2 and 3 for all studied conditions due to a shorter bubble residence time in section 1. In addition, there are two points to notice in Figure 7 regarding the difference between ε_1 and ε_2 (or ε_3) as a function of fiber mass fraction. First, when $0 \leq C \leq 0.4\%$, the difference between ε_1 and ε_2 (or ε_3) at U_g = 5 is very similar to that at 18 cm/s. However, when $C \geq 0.6\%$, the difference is smaller at U_g = 5 cm/s. This is because that at $C \geq 0.6\%$, bubble entrainment at the column exit and backmixing is significant, and it is more evident at higher superficial gas velocities. Second, the difference between ε_1 and ε_2 (or ε_3) increases when C increases from 1.2% to 1.5% at both high and low superficial gas velocities. This is because at a fiber mass fraction as high as 1.5%, the gas-fiber slurry in section 1 is not fully mixed, resulting in temporary channeling or preferential paths of bubble movement, which makes the gas holdup decrease sharply in section 1, as indicated in Figure 7. However, the gas-fiber mixture in sections 2 and 3 are still well mixed; thus, the difference $\varepsilon_2 - \varepsilon_1$ increases.

Gas flow regime transition

In this section, the Zuber-Findlay drift-flux model,[38] which is widely recommended for modeling gas holdup in bubble columns,[13,39–41] is used to identify the gas flow regime transitions. This model accounts for the radial nonuniformity of flow and holdup profiles typically encountered in the heterogeneous flow regime. The drift-flux (j_{gl}) is defined by Wallis[42] as the volumetric flux of gas relative to a surface moving at a velocity equal to the total of the superficial gas and liquid velocity. For a cocurrent bubble column, it can be shown that[39]

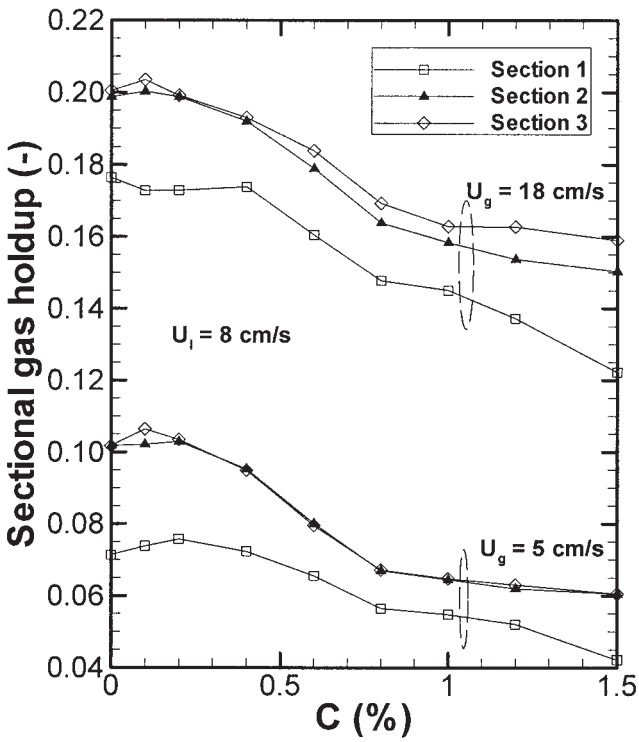

Figure 7. Influence of fiber mass fraction on gas holdup in different column sections.

$$\frac{U_g}{\varepsilon} = C_0(U_g + U_l) + \frac{j_{gl}}{\varepsilon} \tag{2}$$

where C_0 is a distribution parameter gauging the uniformity in the radial velocity and holdup profiles and j_{gl}/ε is a weighted average drift velocity accounting for local slip. The weighted average drift velocity is usually assumed as the terminal bubble rise velocity ($U_{b\infty}$) in an infinite medium because the local slip velocity U_{gl} ($=U_g - U_l$) changes little over the pipe diameter and $j_{gl} = U_{gl}(1 - \varepsilon)$, with $\varepsilon < 0.25$ in most situations for bubble flows.[43] C_0 can be found by plotting U_g/ε as a function of ($U_g + U_l$). For a given gas flow regime, C_0 and $U_{b\infty}$ are constant because the radial velocity, gas holdup distribution, and average bubble size do not change significantly. Zahradnik et al.[40] observed that changes in the slope of the drift-flux plot indicate changes in flow regime. Xie et al.[13] showed that the Zuber-Findlay model could successfully model the gas holdup data in a cocurrent air-water-fiber bubble column, when the flow regime is other than dispersed bubbly flow or layered bubbly flow. Using this method, Su and Heindel[15] demarcated the superficial gas velocities at which flow regime transitions occurred in a 15.24 cm semibatch air-water-Rayon fiber bubble column.

Equation 2 can be rewritten as

$$\frac{U_g}{\varepsilon} = C_0(U_g + U_l) + \frac{j_{gl}}{\varepsilon} = C_0U_g + B_0 \tag{3}$$

where $B_0 = C_0U_l + j_{gl}/\varepsilon$ is a constant for a given flow regime and U_l. We can plot U_g/ε vs. U_g and get the same slope as the U_g/ε vs. ($U_g + U_l$) plot for the same flow conditions. Thus, we can use the U_g/ε vs. U_g plot to identify the superficial gas velocity at which flow regime transition occurs for a given U_l.

Figure 8 shows the effect of fiber mass fraction on U_g/ε as a function of U_g at $U_l = 8$ cm/s. When $C \leq 0.4\%$, the U_g/ε vs. U_g curves can be divided into 3 regions by their slope. According to visual observations and the flow regimes described by Chen et al.[30] and Reese et al.,[16] the 3 regions correspond to dispersed bubble flow (region a), vortical-spiral flow (region b), and turbulent flow (region c). Each of the three regions on one of the U_g/ε vs. U_g curves has the same slope as the counterparts on the other curves. The transition from dispersed bubble flow to vortical-spiral flow occurs at $U_g \approx 4$ cm/s, while the transition from vortical-spiral flow to turbulent flow occurs at $U_g \approx 13\sim14$ cm/s. The boundaries between neighboring flow regimes are different from results in Reese et al.,[16] which is attributed to the difference in column size and gas distribution method. The slope of the vortical-spiral flow is slightly different from that of the turbulent flow while both of them are distinctly different from that of the dispersed bubble flow. When $C \geq 0.6\%$, there is only one gas flow regime transition on the curves, which occurs at $U_g \approx 13\sim14$ cm/s, with a slightly lower U_g corresponding to a higher C. The region where U_g is lower than the transition velocity is vortical-spiral flow while turbulent flow occurs at higher U_g values. The dispersed bubble flow does not appear. The disappearance of the dispersed bubble flow when $C \geq 0.6\%$ is attributed to the enhancement of bubble coalescence by the fiber network.

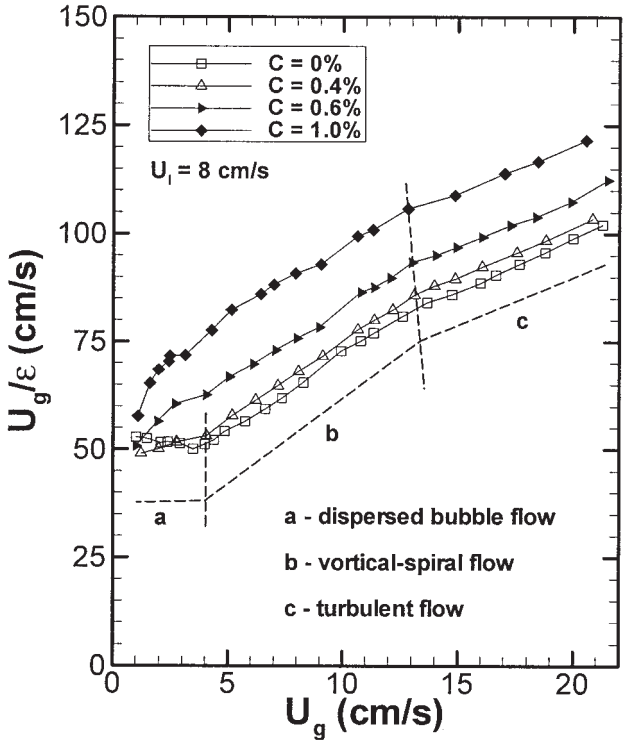

Figure 8. Variation of U_g/ε with superficial gas velocities at different fiber mass fractions ($U_l = 8$ cm/s).

This is consistent with the observations of Reese et al.[16] and Heindel[18] in semibatch bubble columns. When $U_g \gtrsim 5$ cm/s, slopes of the two regions of the U_g/ε vs. U_g curves are independent of C and very close to those of regions b and c for $C \leq 0.4\%$, respectively. When $U_g \lesssim 5$ cm/s and $C \geq 0.6\%$, the slopes increase with C, and are greater than the slope at higher U_g. This is attributed to gas entrainment, which composes a significant fraction of the measured gas holdup at $U_g \lesssim 5$ cm/s and $C \geq 0.6\%$. For example, at $C = 1.0\%$, the entrained gas fraction is estimated to be ~25% of the total gas holdup when $U_g = 0.52$ cm/s and $U_l = 10$ cm/s, and ~8% when $U_g = 5.1$ cm/s and $U_l = 10$ cm/s. Data at other fiber mass fractions[31] reveal the separation distance between neighboring U_g/ε vs. U_g curves varies nonuniformly with C, suggesting that the intercept B_0 in Eq. 3 is a nonlinear function of C.

The results presented in Figure 8 apply at fiber mass fractions up to 1.5%. At $C = 2.0\%$, the general trend is not followed due to significant gas entrainment in fiber suspensions, a large fraction of which circulates with the water-fiber slurry in the system.[31]

Additional data can be found in Tang[31] and suggest that the effect of superficial liquid velocity on flow regime transition and slope is negligible. The superficial liquid velocity only influences the intercept at $U_g = 0$, which is consistent with Eq. 3.

Conclusions

This study examined the effects of superficial liquid velocity, superficial gas velocity, and fiber mass fraction on the gas

holdup and flow regime transition in well-mixed water-fiber suspensions in a 15.24 cm cocurrent bubble column.

Experimental results showed that gas holdup decreases linearly with increasing superficial liquid velocity when fiber mass fraction and superficial gas velocity are constant. Gas holdup was not significantly affected by fiber mass fraction in the range of $C \leq 0.2\%$, but decreased with C in the range of $0.4\% \leq C \leq 1.5\%$. Various mechanisms influenced the effects of superficial liquid velocity and fiber mass fraction on the hydrodynamics and gas holdup, and they were discussed. Interactions between superficial liquid velocity and fiber mass fraction were found to be significant. By comparing this study with previous investigations, gas distribution methods were determined to cause significant differences between the hydrodynamics, and gas holdup in different cocurrent air-water-cellulose fiber bubble column systems.

The axial gas holdup distribution was shown to be a complex function of U_g, U_l, and C. The drift-flux model was used to analyze the flow regime transitions at different operating conditions. Three distinct flow regimes, that is, dispersed bubble flow, vortical-spiral flow, and turbulent flow, were observed when $C \leq 0.4\%$, but only the latter two regimes were identified when $0.6\% \leq C \leq 1.5\%$. The critical superficial gas velocities at which the regime transitions occurred were not significantly affected by U_l and slightly decreased with C.

Acknowledgments

Portions of this project were supported by the National Research Initiative of the USDA Cooperative State Research, Education and Extension Service, grant number 2001-35103-11259. The fiber supply and characterization was provided by Kimberly-Clark Corporation; their support is appreciated.

Literature Cited

1. Heindel TJ. A review of gas flows in fiber suspensions. *TAPPI J.* 2003; 2(11): 22.
2. Bennington CPJ, Kerekes RJ, Grace JR. The yield stress of fiber suspensions. *C J of Chem Eng.* 1990; 68: 748–757.
3. Kerekes RJ. Characterizing fiber suspensions. *Proc of TAPPI 1996 Eng Conf;* September 16–19, 1996; Chicago, IL; 21–28.
4. Kerekes RJ, Soszynski RM, Tam Doo PA. The flocculation of pulp fibers. In: Punton V, ed. Papermaking Raw Materials, Transactions of the 8th Fundamental Research Symposium Held at Oxford: September 1985. Vol 1. London, England: Mechanical Engineering Publications Limited; 1985; 265–310.
5. Robertson AA, Mason SG. Flocculation in flowing pulp suspensions. *Pulp and Paper Magazine of Canada.* 1954; 55: 263–269.
6. Kerekes RJ. Pulp flocculation in decaying turbulence: a literature review. *J of Pulp and Paper Sci.* 1983; 9: TR86–TR91.
7. Norman BG, Moller K, Duffy GG. Hydrodynamics of papermaking fibers in water suspension. *Fiber-Water Interaction in Papermaking, Transactions of the Symposium Held at Oxford.* London, England: British Paper and Board Industry Federation; 1978; 195–249.
8. Steen M. On turbulent structure in vertical pipe flow of fiber suspensions. *Nordic Pulp and Paper Res J.* 1989; 4: 244–252.
9. Andersson SR, Rasmuson A. Flow measurements on a turbulent fiber suspension by laser Doppler anemometry. *AIChE J.* 2000; 46: 1106–1119.
10. Forgacs OL, Robertson AA, Mason SG. The hydrodynamic behaviour of paper making fibers. In: Bolam F, ed. Fundamentals of Papermaking Fibers, Transactions of The Symposium Held at Cambridge, 1957. Surrey, England: Technical Section of BP&BMA; 1958; 447–479.
11. Lindsay JD, Ghiaasiaan SM, Abdel-Khalik SI. Macroscopic flow structures in a bubbling paper pulp-water slurry. *Ind Eng Chemistry Res.* 1995; 34: 3342–3354.
12. Schulz TH, Heindel TJ. A study of gas holdup in a cocurrent air/water/fiber system. *TAPPI J.* 2000; 83(6): 58–59.
13. Xie T, Ghiaasiaan SM, Karrila S, McDonough T. Flow regimes and gas holdup in paper pulp-water-gas three-phase slurry flow. *Chem Eng Sci.* 2003; 58: 1417–1430.
14. Went J, Jamialahmadi M, Muller-Steinhagen H. Effect of wood pulp fibre concentration on gas hold-up in bubble columns. *Chemie Ingenieur Technik.* 1993; 65: 306–308.
15. Su X, Heindel TJ. Gas holdup in a fiber suspension. *C J of Chem Eng.* 2003; 81: 412–418.
16. Reese J, Jiang P, Fan L-S. Bubble characteristics in three-phase systems used for pulp and paper processing. *Chem Eng Sci.* 1996; 51: 2501–2510.
17. Walmsley MRW. Air bubble motion in wood pulp fiber suspension. *APPITA 46th Annual General Conference Proceedings; April, 1992; Launceston, Australia, 509–515.*
18. Heindel TJ. Gas flow regime changes in a bubble column filled with a fiber suspension. *C J of Chem Eng.* 2000; 78: 1017–1022.
19. Heindel TJ, Monefeldt JL. Observations of the bubble dynamics in a pulp suspension using flash x-ray radiography. *TAPPI J.* 1998; 81(11): 149–158.
20. Merchuk JC, Stein Y. Local hold-up and liquid velocity in air-lift reactors. *AIChE J.* 1981; 27: 377–388.
21. Kumar SB, Dudukovic MP, Toseland. Measurement techniques for local and global fluid dynamic quantities in two and three phase systems. In: Chaouki J, Larachi, F., and Dudukovic, M.P., ed. *Non-Invasive Monitoring of Multiphase Flows.* New York, NY: Elsevier; 1997; 1–45.
22. Hills JH. The operation of a bubble column at high throughputs. *Chem Eng J.* 1976; 12: 89–99.
23. Heindel TJ. Bubble size in a cocurrent fiber slurry. *Ind & Eng Chemistry Res.* 2002; 41: 632–641.
24. Maier CG. *Producing small bubbles of gas in liquids by submerged orifices.* Washington, DC: US Bureau of Mines; 1927. Bulletin No. 260.
25. Johnson BD, Gershey RM, Cooke RC, Sutcliffe WH. A theoretical model for bubble formation at a frit surface in a shear field. *Sep Sci and Technol.* 1982; 17: 1027–1039.
26. Waldie B, Johnston T, Harris WK, Bell C. Bubble characteristics in a high-intensity gas/liquid contactor. *Chem Eng Sci.* 1999; 54: 5319–5327.
27. Forrester SE, Rielly CD. Bubble formation from cylindrical, flat and concave sections exposed to a strong liquid cross-flow. *Chem Eng Sci.* 1998; 53: 1517–1527.
28. Hudson K, Kazem B, inventors; Hydro Dynamics, Inc., Rome, GA, assignee. Highly efficient method of mixing dissimilar fluids using mechanically induced cavitation. US patent 6,627,784 B2. September 30, 2003.
29. Tzeng J-W, Chen RC, Fan L-S. Visualization of flow characteristics in a 2-D bubble column and three-phase fluidized bed. *AIChE J.* 1993; 39: 733–744.
30. Chen RC, Reese J, Fan L-S. Flow structure in a three-dimensional bubble column and three-phase fluidized bed. *AIChE J.* 1994; 40: 1093–1104.
31. Tang C. *Hydrodynamics and Gas Holdup in a Cocurrent Air-Water-Fiber Bubble Column* Ph.D. Thesis. Ames, IA: Department of Mechanical Engineering, Iowa State University; 2005.
32. Ajersch M, Pelton R. The behavior of air bubbles in aqueous wood pulp suspensions. *Proc. of the 5th Res. Forum on Recylcing;* September 28–30, 1999; Ottawa, Ont, Canada, 97–112.
33. Heindel TJ. Bubble size measurements in a quiescence fiber suspension. *J of Pulp and Paper Sci.* 1999; 25: 104–110.
34. Clift R, Grace JR, Weber ME. *Bubbles, Drops, and Particles.* New York, NY: Academic Press, 1978.
35. Hesketh RP, Etchells AW, Russell TWF. Bubble breakage in pipeline flow. *Chem Eng Sci.* 1991; 46: 1–9.
36. Risso F. The mechanisms of deformation and breakup of drops and bubbles. *Multiphase Sci and Technol.* 2000; 12: 1–50.
37. Walter JF, Blanch HW. Bubble break-up in gas-liquid bioreactors: break-up in turbulent flows. *Chem Eng J.* 1986; 32: B7–B17.
38. Zuber N, Findlay JA. Average volumetric concentration in two-phase flow systems. *J of Heat Transfer.* 1965; 87: 453–468.

39. Shah YT, Kelkar BG, Godbole SP, Deckwer WD. Design parameters estimations for bubble column reactors. *AIChE J.* 1982; 28: 353–379.
40. Zahradnik J, Fialova M, Ruzicka M, Drahos J, Kastanek F, Thomas NH. Duality of the gas-liquid flow regimes in bubble column reactors. *Chem Eng Sci.* 1997; 52: 3811–3826.
41. Ruzicka MC, Zahradnik J, Drahos J, Thomas NH. Homogeneous-heterogeneous regime transition in bubble columns. *Chem Eng Sci.* 2001; 56: 4609–4626.
42. Wallis GB. *One-dimensional Two-phase Flow*. New York: McGraw-Hill, 1969.
43. Clark NN, van Egmond JW, Nebiolo EP. The drift-flux model applied to bubble columns and low velocity flows. *Intal J of Multiphase Flow*. 1990; 16: 261–279.

Manuscript received June 2, 2004, and revision received Dec. 22, 2004.